Performance of Glasses Containing Titan as Potential Corrosion Inhibitors for Mild Steel in a 3% NaCl Solution

A. Shaim[1], Galai M[1]*, K. Ba[1], K. Dahmani[2], A. Chahine[1], D. Rair[1], M. Ebn Touhami[1] and A. Benlhachemi[2]

[1]*Advanced Materials and Process Engineering Laboratory, Faculty of Sciences, Ibn Tofail University, Kenitra, Morocco*
[2]*Materials and Environment Laboratory, Faculty of Sciences, Ibn Zohr University, Agadir, Morocco*
*Corresponding author: galaimouhsine@gmail.com

Received 18/01/2022; accepted 05/05/2022
https://doi.org/10.4152/pea.2023410503

Abstract
Inhibition of MS corrosion in a 3% NaCl solution, by glasses containing Ti-0, Ti-5 and Ti-7, in different C, was investigated using AFM, EIS, FTIR spectroscopy, PPD, SEM and XRD techniques. PPD and IES gave IE(%) of 92.8, 99 and 98.3%, and 91.9, 98 and 98.3%, for Ti-0, Ti-5 and Ti-7 glasses, respectively, at optimum C (0.4 g/L). In addition, EIS results indicated that IE(%)increased with higher C of Ti in the glasses, reaching its maximum at 7% TiO_2. The three studied compounds acted as anodic inhibitors, though anodic reactions were more suppressed than the cathodic ones. SEM revealed that the inhibitors significantly stopped the attack by Cl^- ions, through chemical adsorption onto the MS surface.

Keywords: Ti-0, Ti-5 and Ti-7 glasses; MS; 3% NaCl; AFM; EIS; FTIR; PPD; SEM; XRD.

Introduction•

MS is the most widely used Fe alloy in industries. It comes very frequently in contact with Cl^- ions, under numerous conditions and circumstances [1]. Cl^- ions are known to be aggressive towards MS, causing severe corrosion problems. Various inorganic compounds, e.g., nitrates, sulfates, silicates and chromates, have been reported as inhibitors of MS corrosion in water containing Cl^-, but their IE(%), when used by themselves, was found to be very low [2-4]. Zn^{2+}, as inhibitor of steel corrosion in water, has been known since the 19th century, with many examples of its use in combination with other compounds, in order to improve metals protection [5-9]. Zn salts relatively low toxicity and ready availability have led to their wide use in practice.

Many organic composites with N, S and P atoms have also been examined as corrosion inhibitors for Fe dissolution in acidic and halide media [10-13].

• The abbreviations and symbols definition lists are in pages 356-357.

Compounds containing P, such as phosphonates and polyphosphates [14, 15], have also been included among such inhibitors. In fact, such composites, in combination with Zn^{2+}[16-19], have shown synergistic effects, and can provide high IE(%) for MS corrosion in water containing Cl^-. In various industries, water is in great demand, and its largest source is sea water, which has high corrosivity, due to the presence of approx. 3.5% NaCl [20-24]. Moreover, MS, the cheapest and more applicable material in industries, gets attacked by Cl^-. So, it becomes a basic need to investigate various corrosion inhibitors for MS in 3% NaCl solutions [25-30].

Experimental procedure

Electrochemical cell

The electrolysis cell was a borosilicate glass (Pyrex®) cylinder closed by cap, with three apertures. The used WE was MS, and its chemical composition is summarized in Table 1. The investigated surface had 1 cm^2. Before each experiment, MS was polished using emery paper until 1500 grade, cleaned with ethanol, washed with distilled water and dried at room T. MS, Pt and SC were used as WE, CE and RE, respectively. For long exposure experiments, between two measurements, the RE was washed from the test solution, for minimizing its contamination by Cl^-, and the WE was set in immersion for 30 min, before each test. Also, the three Ti glasses were very soluble in a NaCl solution.

Table 1. MS chemical composition (wt%).

C	Si	Mn	Cr	Mo	Ni	Al	Cu	Co	V	W	Fe
0.11	0.24	0.47	0.12	0.02	0.1	0.03	0.14	<0.0012	<0.003	0.06	Balance

Glasses preparation

The glasses were elaborated by direct melting of $NaPO_3$ and TiO_2, with the compositions (100-x) $NaPO_3$-x TiO_2 (x = 0, 5 and 7% mol), in stoichiometric proportions. The reagents were finely ground in an agate mortar, and then placed in a porcelain crucible. Two thermal stages for minimizing P_2O_5 evaporation, at 300 and 700 ºC, during 1 and 2 h, respectively, were achieved. The melting T (1100 ºC) of the most refractory composition was used as the preparation T for the entire composition series of this system. Finally, after heating at the preparation T, for 30 min, the glasses were poured into a SS plate.

Polarization measurements

The WE was immersed in a 3% NaCl solution, during 30 min, until the E_{corr} steady state was reached. The cathodic polarization curve was recorded from E_{corr}, towards a negative direction, with a SR of 1 mV/s. After this scan, the WE was kept in the solution, until the steady state E_{corr} (±0.02 V) was reached. The anodic polarization curve was recorded from $E_{corr,}$ towards a positive direction, also at 1 mV/s. The obtained polarization curves were corrected for ohmic drop, and the electrolyte resistance was determined by EIS. These measurements were carried out using a PGZ100 potentiostat monitored by a personal computer. For each C, three independent experiments were performed. The mean values and SD were also

reported. However, the overall i_{corr} was considered as the sum of two contributions, i_a and i_c. For the domain not too far from OCP, we can consider that both processes obeyed the Tafel law (Eq. 1) [2, 31]:

$$i = i_a + i_b = i_{corr} \times \left(e^{b_a \times (E - i_{corr})} - e^{b_c \times (E - E_{corr})}\right) \quad (1)$$

where i_{corr},. β_a and β_c are expressed in A/cm^{-2} and V^{-1}, respectively. These constants are related to β (V/dec^{-1}), in a usual logarithmic scale, by the following equation:

$$\beta = \frac{\ln(10)}{b} = \frac{2.303}{b} \quad (2)$$

The corrosion parameters were then evaluated by the NLS method, with EC-Lab software, applying that equation. However, for this calculation, the applied E range was limited to ±0.100 V around E_{corr}. Thus, a significant systematic divergence was sometimes observed for both anodic and cathodic branches. IE(%) was calculated using the following equation [2]:

$$IE(\%) = \left[1 - \frac{i_{corr}}{i^{\circ}_{corr}}\right] \times 100 \quad (3)$$

where i°_{corr} and i_{corr} are represent values without and with inhibitors, respectively.

EIS measurements

EIS measurements were carried out using a transfer function analyzer (Voltalab PGZ100, Radiometer Analytical), over the frequency range from 100 kHz to 100 mHz, with 10 points per decade. The amplitude of the AC signal was 10 mV_{rms}. All experiments were performed at OCP. The obtained impedance data were analyzed in terms of the equivalent electrical circuit, using Bouckamp's program [32]. IE(%) applied was evaluated from R_p (which was obtained from the semicircle diameter in Nyquist representation), with the following equation [33]:

$$\eta = \left[1 - \frac{R_p^0}{R_p}\right] \times 10 \quad (4)$$

where R°_p and R_p represent values without and with inhibitors, respectively.

Surface studies

In order to support electrochemical results, surface morphological SEM was used for the MS specimens immersed in a 3% NaCl solution, during 24 h, without and with Ti glasses.

Results and discussion

FTIR analysis

The infrared spectra of the Ti glasses system, in the frequency range from 400 to 1400 cm^{-1}, are shown in Fig. 1.

The different spectra are composed of broad lines that are typical of amorphous systems.

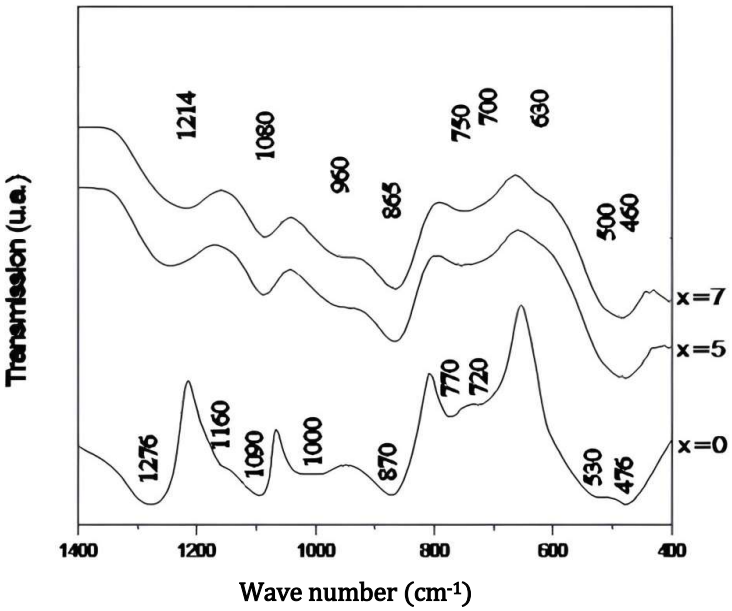

Figure 1. FTIR spectra of the Ti glasses system with the composition $(50-\frac{x}{2})Na_2O–xTiO_2–(50-\frac{x}{2})P_2O_5 (0 \leq x \leq 7$ % molar $TiO_2)$.

The plot, representative of $NaPO_3$ ($50Na_2O$ - $50P_2O_5$) (x = 0) is consistent with data reported in the literature on this type of composition [34]. We found AVV and SVV of the PO_2 groups at 1276 and 1160 cm^{-1}, respectively, which are characteristic of highly condensed phosphates. The absorptions at 1090 and 1000 cm^{-1} correspond to AVV and SVV of the PO_3 groups (terminal groups), respectively. The bands located around 870 and 750 cm^{-1} (doublet) are attributed to AVV and SVV absorptions of the P-O-P bonds, respectively. All the deformation vibrations of PO_4 are grouped in the area from 530 to 470 cm^{-1}.

The spectra corresponding to the glasses containing Ti (x = 0, 5 and 7) show absorption bands typical of $NaPO_3$ glass. However, the band attributed to the AVV of PO_2 shifted from 1276 cm^{-1}, for the $NaPO_3$ glass, to 1214 cm^{-1}, for the $(45)Na_2O$-$10TiO_2$-$(45)P_2O_5$ composition. This result was expected, since the phosphate chains interact more strongly with Ti than with Na and, therefore, the P-O bonds that bind with Ti ions are longer than those that bind with Na ions.

Along with the shift in the bands related to AVV of PO_2, the intensities of the absorption bands corresponding to AVV of O-P-O and SVV of P-O-P decreased with higher TiO_2 content. These changes in the spectra of glasses with higher TiO_2 C were due to a decrease in the length of the phosphate chains [35].

$NaPO_3$ depolymerization by TiO_2 led to the formation of short phosphate chains, characterized by the appearance of the AVV of PO_2 at 1214 cm^{-1}. Indeed, this band appears at 1000-1240 cm^{-1} in $P_4O_{13}^{6-}$, and at 1215 cm^{-1} in $Na_5P_3O_{10}$ [34].

XRD

In order to confirm the amorphous nature of our processed samples, XRD was performed. The recorded curves (Fig. 2) do not show diffraction peaks on our synthesized glass samples, but they show diffuse and broad peaks characteristic of the glassy state.

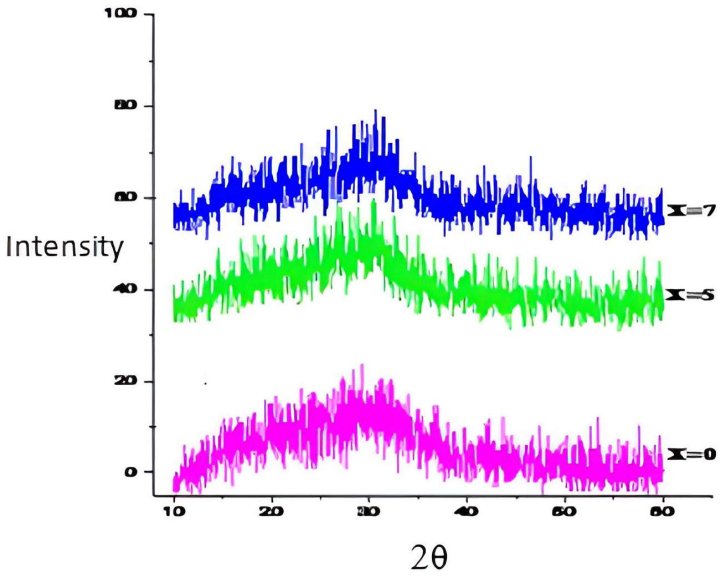

Figure 2. XRD spectra of the glass samples.

PDP

PDP curves of MS in the 3% NaCl solution without and with the three inhibitors, in various C, are presented in Fig. 3.

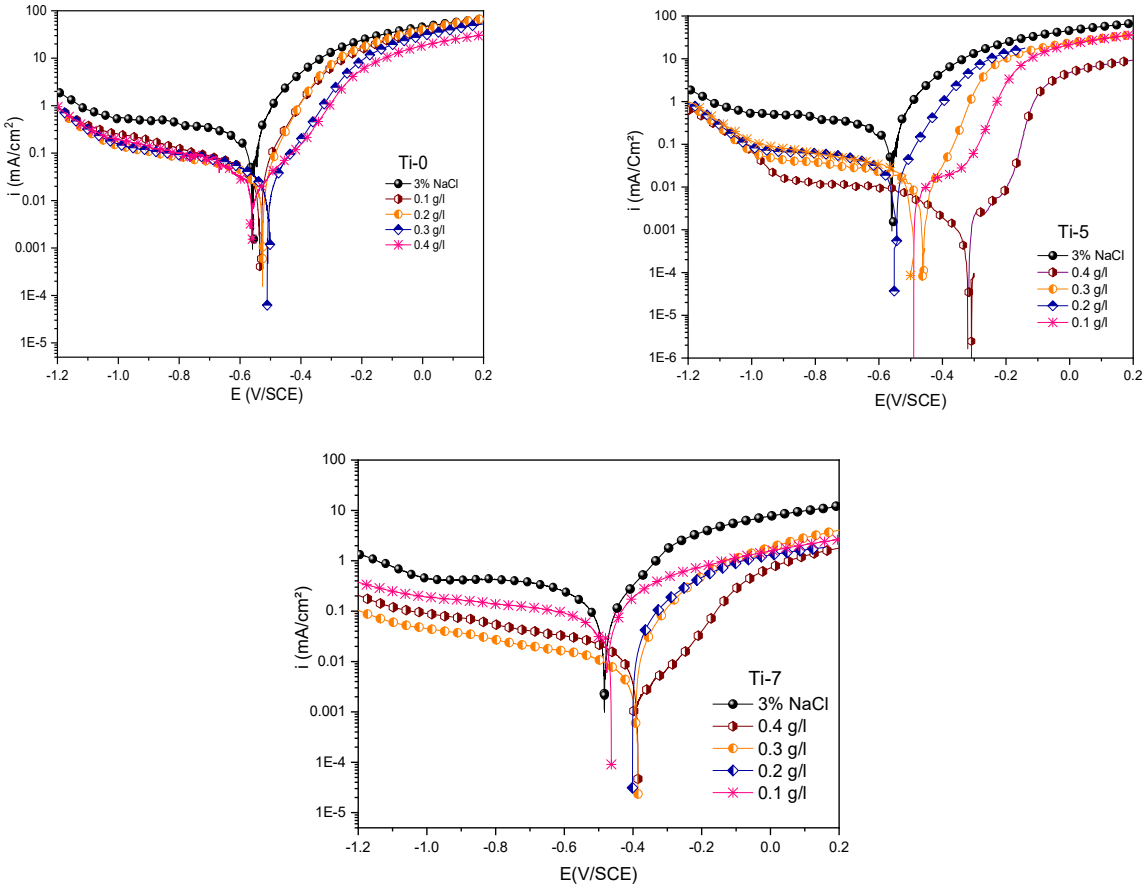

Figure 3. PDP curves of MS in 3% NaCl without and with Ti-0, Ti-5 and Ti-7, in different C.

The C range of Ti-0, Ti-5 and Ti-7 was from 0.1 to 0.4 g/L. All these curves were obtained after 1 h of immersion of the electrode in the electrolytic solution at OCP E_{corr} [36, 37]. Then, cathodic and anodic polarization curves were recorded from independent experiments. For the cathodic and anodic scans, the initial E values were slightly more positive and negative, respectively, from E_{corr}.
From polarization diagrams shown in Fig. 3, it is evident that the inhibitors suppressed both cathodic and anodic reactions. Table 2 shows that Ti-0, Ti-5 and Ti-7, at the optimum C of 0.4 g/L, reached the highest IE(%) values of 92.8, 99 and 98.3%, respectively, and it also displays parameters, such as E_{corr}, i_{corr}, β_c and β_a, derived through the extrapolation method. β_c values for the inhibitors changed with higher C than those of the blank solution, which suggests their effect on the kinetics of H_2 release. When Ti-0, Ti-5 and Ti-7 C were raised to 0.4 g/L, β_a values decreased to 110, 8.83 and 104 mV/dec^{-1}, respectively [38-40].This implies that the kinetics of Fe dissolution in 1 M HCl was modified by these compounds, during the protection process, which can be attributed to their adsorption onto the MS surface active centers. The i_{corr} values decreased with higher C of the inhibitors in 1 M HCl, reaching their lowest values at 0.4 g/L [41-44].

Table 2. Electrochemical parameters for MS in NaCl 3% containing different inhibitors C.

Medium	Conc. (g /L)	E_{corr} (mV/SCE)	i_{corr} ($\mu A/cm^{-2}$)	β (mV/dec)		IE (%)
				$-\beta_c$	βa	
3% NaCl	-	559	280	121	121	-
Ti-0	0.1	532	37	177	119	86,7
	0.2	524	35	158	97	87,5
	0.3	499	22	176	104	92,1
	0.4	558	20	145	110	92,8
Ti-5	0.1	498	27	2.48	10.2	90
	0.2	594	40	12	9	85
	0.3	463	14	4.64	7.93	94
	0.4	320	3	10.84	8.83	99
Ti-7	0.1	478	22	73	138	92
	0.2	404	14	75	142	95
	0.3	394	12	95	120	95.6
	0.4	390	5	101	104	98.3

Tafel plots revealed that, with the increase in the three compounds C, anodic and cathodic i_{corr} decreased, E_{corr} shifted to more positive values, and both cathodic and anodic β were affected. These results confirm the inhibitor anodic activity. Accordingly, E_{corr} shifted to the cathodic branch direction, but the changes in the anodic β were more significant, implying the inhibitor role on the anodic MS dissolution mechanism. The lowest i_{corr} value was obtained at the highest inhibitors C. The polarization data revealed that 0.4 g/L of the three inhibitors offered higher corrosion IE(%) than that of other C. These results showed the high capability of Ti glass inhibitors for MS CR reduction, through adsorption and/or film formation on the active sites [34, 45].

EIS

MS specimens were immersed in the 3 wt% NaCl solutions with and without the three inhibitors, and their influence on the corrosion IE(%) of the samples was investigated by EIS. Fig. 4 shows the Nyquist plots for the various MS samples, which exhibited larger semicircles for the solutions with inhibitors than for those without them.

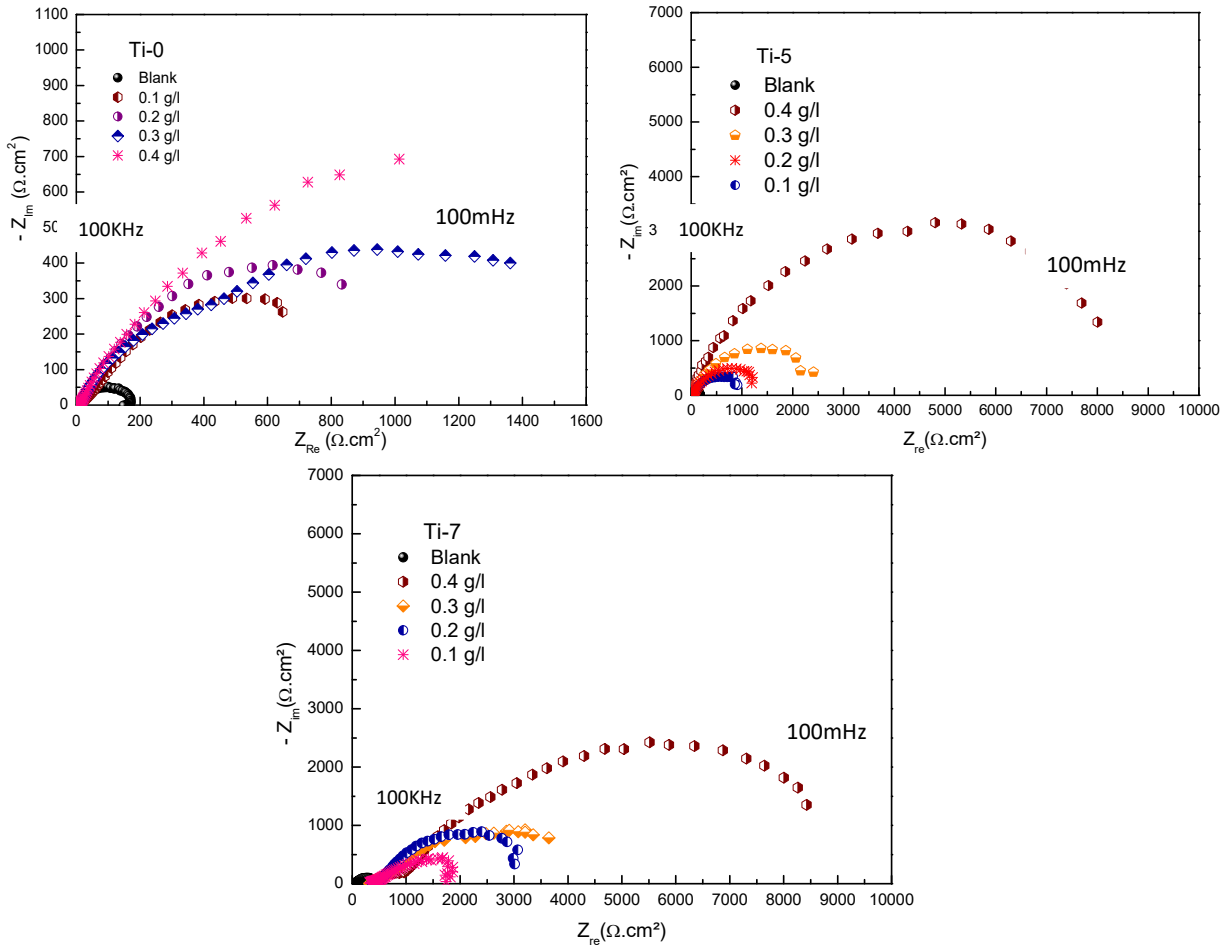

Figure 4. Nyquist diagrams for MS without and with Ti-0, Ti-5 and Ti-7, in different C, after 30 min of immersion.

In the case of brass, equivalent circuits (Fig. 5) were connected in series with two times constants. CPE means the possibility of a non-ideal capacitance, where n is the variable. CPE impedance is given by the following equation [35, 46]:

$$Z_{CPE} = \frac{1}{A(i\omega)^n} \qquad (5)$$

where A is CPE magnitude, ω is the sine wave modulation angular frequency, 1 is the imaginary number and n is an empirical exponent that measures the deviation from the ideal capacitive behavior. Depending on n values (0, 1, -1 and 0.5), CPE can represent resistance, capacitance, inductance and Warburg impedance, respectively. [47]. The C_{dl} values derived from CPE and τ of the charge-transfer process, can be calculated using eqs. 6 and 7, respectively [48].

$$C_{dl} = \sqrt[n]{A(R_{ct})^{1-n}} \quad (6)$$

$$\tau = R_{ct} \times C_{dl} \quad (7)$$

The proposed electrical circuit, as shown in Fig. 5, was used to describe the MS /electrolyte interface model. The employed circuit allowed for the identification of R_s, R_{ct} and R_f. It is noteworthy that the C_{dl} value was affected by imperfections on the surface, and this effect was simulated via CPE [49, 50]. Q_{ct} and n parameters were employed when the surface heterogeneity could affect them. This heterogeneity might be due to surface roughness, corrosion product adsorption and porous layer formation. Therefore, the expression differs from CPE impedance frequently used nowadays, where the impedance of parallel connection between CPE and R_s will be expressed as [51]:

$$Z_{CPE} = \frac{Rs}{1 + Rs \times CPE(j\omega)^n} \quad (8)$$

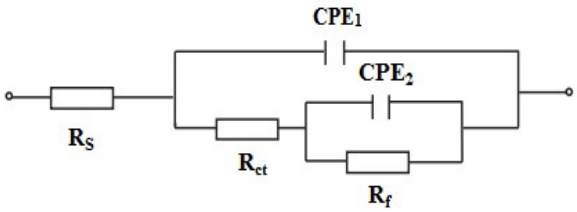

Figure 5. Electrochemical equivalent circuit used to fit impedance spectra.

Table 3. Electrochemical impedance parameters for MS corrosion in 3%NaCl with various C of Ti-0, Ti-5 and Ti-7.

Inhibitors	C (g/L)	R_s (Ω/cm²)	Q_f (µF/cm²)	n_f	R_f (KΩ/cm²)	Q_{ct} (µF/ cm²)	n_{ct}	R_{ct} (KΩ/ cm²)	R_p (KΩ/ cm²)	IE(%)
3% NaCl	-	10	-	-	-	-	-	0.175	0.165	-
Ti-0	0.1	11	3145	0.706	0.522	2057	0.937	0.676	1.187	86.1
	0.2	13	3648	0.602	0.258	3600	0.601	0.979	1.224	86.5
	0.3	7	808	0.633	0.932	3198	0.574	1.082	2.007	91.7
	0.4	10	3352	0.724	1.144	7623	1	0.912	2.046	91.9
Ti-5	0.1	15	550	0.70	0.04	30	0.54	1.1	1.1	85
	0.2	12	107	0.67	0.1	146	0.98	1.5	1.6	90
	0.3	12	441	0.68	0.3	72	0.97	2.4	2.7	94
	0.4	8	61	0.85	2.1	75	0.65	6.9	9	98
Ti-7	0.1	32	41	0.52	0.153	495	0.43	1.875	2.028	92
	0.2	31	71	0.6	0.109	491	0.65	3.250	3.359	95
	0.3	32	115	0.52	0.420	203	0.76	4.420	4.840	95.6
	0.4	43	22	0.57	0.707	171	0.63	8.920	9.627	98.3

In the 0.4 g/L inhibited solutions, the impedance responses in the low frequency presented an increasing trend over time. It seems that more inhibiting species were available at the MS surface active zones with higher Ti glasses C up to 0.4 g/L. This means that this C of Ti-0, Ti-5 and Ti-7 in 3% NaCl led to a higher corrosion IE(%). Inspection of the results in Table 3 indicates that R_{ct} value increased with higher inhibitors C. In addition, CPE value varied regularly with the Ti glasses C. The change in R_{ct} and CPE values can be related to the gradual removal of water

molecules by the inhibitors molecules on the MS surface, which led to a decrease in the number of active sites prone to the corrosion reaction [52]. The increase in R_{ct} value was due to the formation of a protective film on the metal/solution interface. The ongoing stability of η (in the range of 0.79-0.93) indicates that MS dissolution mechanism was charge transfer controlled, without and with the inhibitors. Moreover, C_{dl} decreased with higher Ti-0, Ti-5 and Ti-7 C, which was probably caused by a decrease in the local dielectric constant and/or by an increase in the electrical double layer thickness at MS surface. This suggests water molecules replacement (with high dielectric constant) by the inhibitors molecules (with low dielectric constant), which enhanced MS resistance [53]. The thickness of this protective layer was evaluated from the Helmholtz model given by the following equation [54]:

$$C_{dl} = \frac{\varepsilon_0}{e} S \quad (9)$$

where ε_0 is the permittivity of space, ε is the local dielectric constant, e is the film thickness and S is the surface area. Eq. 10 suggests that C_{dl} is inversely proportional to the protective layer thickness. So, the decrease in C_{dl} values resulted in an increase in IE (%) values (Table 3).

SEM analysis

SEM micrographs of MS surfaces after 24 h immersion in 3% NaCl, without and with inhibitors (0.4 g/L), are shown in Fig. 6.

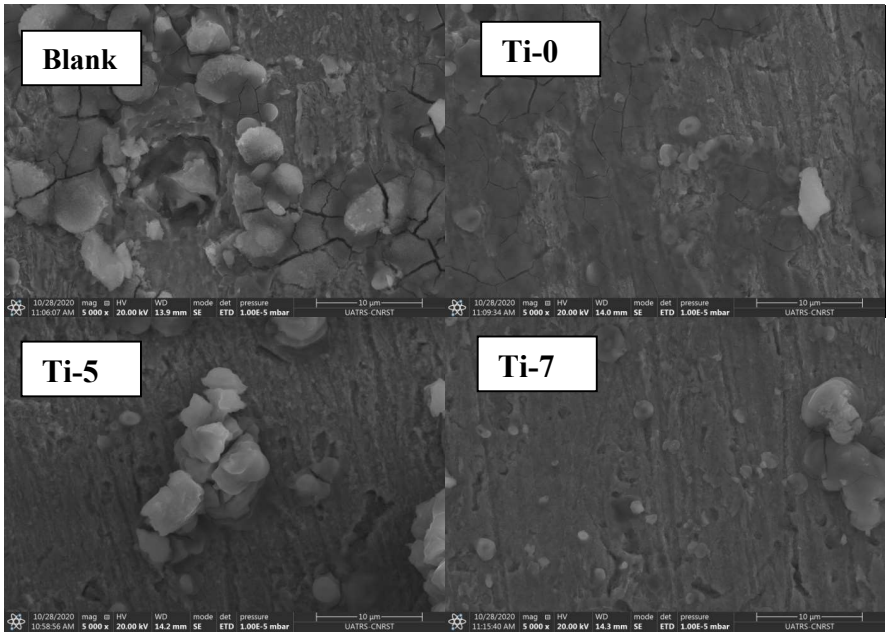

Figure 6. SEM images of MS after 24 h immersion in 3% NaCl without and with Ti-0, Ti-5 and Ti-7 (0.4 g/L).

It can be clearly observed that, without inhibitors, MS surface is highly corroded, due to the NaCl attack. However, with inhibitors, MS surface morphologies remarkably improved [55-60], which suggests that they were adsorbed at the metal-electrolyte interfaces, forming protective films.

Conclusion

Electrochemical studies showed that the tested Ti glasses compounds are good inhibitors of MS corrosion in 3% NaCl. The inhibitors acted simultaneously on the anodic and cathodic electrochemical processes. Polarization curves show that the inhibiting effect of this compound resulted in a clear decrease in the cathodic and anodic i_{corr} values, especially in the vicinity of E_{corr}. A remarkable corrosion inhibition effect of Ti glasses was observed when their C was 0.4 g/L. Their IE(%) depended on the vitreous phase composition, reaching its higher value (98%) at 0.4 g/L and 7% TiO_2. The impedance tests confirmed these results and revealed that the inhibitor addition effect was seen as an increase in R_{ct}, and as a strong decrease in electrochemical interface capacity value. The studies of the examined compounds adsorption onto the MS surface were reinforced by SEM, EDS and AFM. All these analyses led the authors of the present study to propose the formation of a strong inhibiting film that passivated MS, with very low i_{corr} values.

Authors' contributions

A. Shaim: wrote the paper. **M. Galai**: collected the data. **A. K. Ba**: conceived and designed the analysis. **K. Dahmani**: conceived and designed the analysis. **A. Chahine**: collected the data. **D. Rair**: performed the analysis. **M. Ebn Touhami**: collected the data. **A. Benlhachemi**: inserted data or analysis tools.

Abbreviations

AC: alternating current
AFM: atomic force microscopy
AVV: antisymmetric valence vibrations
C: concentration
C_{dl}: double layer capacitance
CE: counter electrode
CPE: constant phase element
CR: corrosion rate
E: potential
E_{corr}: corrosion potential
EIS: electrochemical impedance spectroscopy
FTIR: Fourier transform infrared
I: current density
i_a: anodic current
i_c: cathodic current
i_{corr}: corrosion current density
IE(%): inhibition efficiency
MS: mild steel
n: CPE exponent
n_{ct}: heterogeneity coefficient of charge-transfer electrons
n_f: heterogeneity coefficient of the inhibitors film
$Na_5P_3O_{10}$: sodium tripolyphosphates
NaCl: sodium chloride
$NaPO_3$: sodium hexametaphosphate

NLS: nonlinear least square
OCP: open circuit potential
P_2O_5: phosphorus pentoxide
$P_4O_{13}^{6-}$: tetrapolyphosphates
PDP: potentiodynamic polarization
Q_{ct}: double layer capacitance of MS
Q_f: double layer capacitance of the inhibitors film
R_a: average roughness
R_{ct}: charge transfer resistance
RE: reference electrode
R_f: resistance associated with the layer of products formed
rms: root-mean-square
R_p: polarization resistance
R_s: solution resistance
SC: saturated calomel
SD: standard deviation.
SEM: scanning electron microscopy
SR: scan rate
SS: stainless-steel
SVV: symmetric valence vibrations
T: temperature
WE: working electrode
XRD: X-ray diffraction

Symbols definition

β: Tafel slope
β_a: anodic Tafel constant
β_c: cathodic Tafel constant
τ: relaxation time constant

References

1. Rbaa M, Benhiba F, Hssisou R et al. Green synthesis of novel carbohydrate polymer chitosan oligosaccharide grafted on d-glucose derivative as bio-based corrosion inhibitor. J Mol Liq. 2021;322:114549. https://doi.org/10.1016/j.molliq.2020.114549
2. Galai M, Rbaa M, Ouakki M et al. Chemically functionalized of 8-hydroxyquinoline derivatives as efficient corrosion inhibition for steel in 1.0 M HCl solution: experimental and theoretical studies. Surf Interf. 2021;21:100695. doi.org/10.1016/j.surfin.2020.100695
3. Galai M, Ouassir J, Touhami ME et al. α-Brass and (α+ β) brass degradation processes in Azrou soil medium used in plumbing devices. J Bio- Tribo-Corros. 2017; 3:1-15. https://doi.org/10.1007/s40735-017-0087-y
4. Galai M, El Faydy M, El Kacimi Y et al. Synthesis, characterization and anti-corrosion properties of novel quinolinol on C-steel in a molar hydrochloric acid solution. Port Electrochim Acta. 2017;35:233-251. https://doi.org/10.4152/pea.201704233
5. Kuznetsov YI, Raskol'nikov A. Nitril-trimethyl phosphonate complexes as corrosion inhibitors for iron. Zashchita Metallov. 1992;28:249-256.
6. Telegdi J, Kalman E, Karman F. Corrosion and scale inhibitors with systematically changed structure. Corros Sci. 1992;33:1099-1103.

7. Hsissou R, Benhiba F, Echihi S et al. Performance of curing epoxy resin as potential anticorrosive coating for carbon steel in 3.5% NaCl medium: Combining experimental and computational approaches. Chem Phys Lett. 2021;783:139081. https://doi.org/10.1016/j.cplett.2021.139081
8. Hsissou R, Benhiba F, Echihi S et al. New epoxy composite polymers as a potential anticorrosive coatings for carbon steel in 3.5% NaCl solution: Experimental and computational approaches. Chem Data Coll. 2021;31:100619. https://doi.org/10.1016/j.cdc.2020.100619
9. Hsissou R, Abbout S, Safi Z et al. Synthesis and anticorrosive properties of epoxy polymer for CS in [1 M] HCl solution: Electrochemical, AFM, DFT and MD simulations. Constr Build Mat. 2021;270:121454. https://doi.org/10.1016/j.conbuildmat.2020.121454
10. Ouass A, Galai M, Ouakki M et al. Poly(sodium acrylate) and Poly(acrylic acid sodium) as an eco-friendly corrosion inhibitor of mild steel in normal hydrochloric acid: experimental, spectroscopic and theoretical approach. J Appl Electrochem. 2021. https://doi.org/10.1007/s10800-021-01556-y
11. Dagdag O, Hsissou R, El Harfi A et al. Epoxy resins and their zinc composites as novel anti-corrosive materials for copper in 3% sodium chloride solution: experimental computational studies. J Mol Liq. 2020;315:113757. https://doi.org/ 10.1016/j.molliq.2020.113757
12. Dagdag O, Hsissou R, El Harfi A et al. Development and Anti-corrosion Performance of Polymeric Epoxy Resin and their Zinc Phosphate Composite on 15CDV6 Steel in 3wt% NaCl: experimental computational studies. J Bio-Tribo-Corros. 2020;6:1-9. https://doi.org/10.1007/s40735-020-00407-1
13. Rbaa M, Fardioui M, Verma C et al. 8-Hydroxyquinoline based chitosan derived carbohydrate polymer as biodegradable and sustainable acid corrosion inhibitor for mild steel. Experimental and computational analyses. Int J Bio Macromol. 2020;155:645-655. https://doi.org/10.1016/j.ijbiomac.2020.03.200
14. Lata S, Chaudhary R. Some triphosphates as corrosion inhibitors for mild steel in 3% NaCl solution. 2008.
15. Errahmany N, Rbaa M, Abousalem AS et al. Experimental, DFT calculations and MC simulations concept of novel quinazolinone derivatives as corrosion inhibitor for mild steel in 1.0 M HCl medium. J Mol Liq. 2020;312:113413. https://doi.org/10.1016/j.molliq.2020.113413
16. Suzuki T, Nishihara H, Aramaki K. The synergistic inhibition effect of octylmercaptopropionate and 8-quinolinol on the corrosion of iron in an aerated 0.5 M Na2SO4 solution. Corros Sci. 1996;38:1223-1234. https://doi.org/10.1016/0010-938X(95)00172-G
17. Tazouti A, Errahmany N, Rbaa M et al. Effect of hydrocarbon chain length for acid corrosion inhibition of mild steel by three 8-(n-bromo-R-alkoxy)quinoline derivatives: Experimental and theoretical investigations. J Mol Struct. 2021;1244:130976. https://doi.org/10.1016/j.molstruc.2021.130976
18. Kadiri L, Galai M, Ouakki M et al. *Coriandrum Sativum* l. seeds extract as a novel green corrosion inhibitor for mild steel in 1.0 M hydrochloric and 0.5 M sulfuric solutions. Analyt Bioanalyt Chem. 2018;10:249-268.
19. El Faydy M, Galai M, El Assyry A et al. Experimental investigation on the corrosion inhibition of carbon steel by 5-(chloromethyl)-8-quinolinol hydrochloride in hydrochloric acid solution. J Mol Liq. 2016;219:396-404. https://doi.org/10.1016/j.molliq.2016.03.056

20. Hsissou R, Bekhta A, Elharfi A et al. Theoretical and electrochemical studies of the coating behavior of a new epoxy polymer: hexaglycidyl ethylene of methylene dianiline (HGEMDA) on E24 steel in 3.5% NaCl. Port Electrochim Acta. 2018;36:101-117. https://doi.org/10.4152/pea.201802101
21. Hsissou R, Benzidia B, Hajjaji N et al. Elaboration and electrochemical studies of the coating behavior of a new nanofunctional epoxy polymer on E24 steel in 3.5% NaCl. Port Electrochim Acta. 2018;36:259-270. https://doi.org/10.4152/pea.201804259
22. R. Hssissou, Benzidia B, Hajjaji N et al. Elaboration, electrochemical investigation and morphological study of the coating behavior of a new polymeric polyepoxide architecture: crosslinked and hybrid decaglycidyl of phosphorus penta methylene dianiline on E24 carbon steel in 3.5% NaCl. Port Electrochim Acta. 2019;37:179-191. https://doi.org/10.4152/pea.201903179
23. Molhi A, Hsissou R, Damej M et al. Performance of two epoxy resins against corrosion of C38 steel in 1 M HCl: Electrochemical, thermodynamic and theoretical assessment. Int J Corros Scale Inhib. 2021;10:812-837. https://doi.org/10.17675/2305-6894-2021-10-2-21
24. Abbout S, Hsissou R, Chebabe D et al. Investigation of the anti-corrosion properties of Galactomannan as additive in epoxy coatings for carbon steel: Rheological and electrochemical study. Inorg Chem Commun. 2021;134:108971. https://doi.org/10.1016/j.inoche.2021.108971
25. Hsissou R. Review on epoxy polymers and its composites as a potential anticorrosive coatings for carbon steel in 3.5% NaCl solution: Computational approaches. J Mol Liq. 2021;336:116307. https://doi.org/10.1016/j.molliq.2021.116307
26. El-Aouni N, Hsissou R, Safi Z et al. Performance of two new epoxy resins as potential corrosion inhibitors for carbon steel in 1 M HCl medium: Combining experimental and computational approaches. Coll Surf A: Physicochem Eng Asp. 2021;626:127066. https://doi.org/10.1016/j.colsurfa.2021.127066
27. Echihi S, Hsissou R, Benzbiria N et al. Performance of Methanolic Extract of Artemisia herba alba as a Potential Green Inhibitor on Corrosion Behavior of Mild Steel in Hydrochloric Acid Solution. Biointerf Res Appl Chem. 2021;11:14751-14763. https://doi.org/10.33263/BRIAC116.1475114763
28. Benhiba F, Sebbar N, Bourazmi H et al. Corrosion inhibition performance of 4-(prop-2-ynyl)-[1, 4]-benzothiazin-3-one against mild steel in 1 M HCl solution: Experimental and theoretical studies. Int J Hydrog Ener. 2021;46:25800-25818. https://doi.org/10.1016/j.ijhydene.2021.05.091
29. Benhiba F, Hsissou R, Benzekri Z et al. DFT/electronic scale, MD simulation and evaluation of 6-methyl-2-(p-tolyl)-1,4-dihydroquinoxaline as a potential corrosion inhibition. J Mol Liq. 2021;335:116539. https://doi.org/10.1016/j.molliq.2021.116539
30. Abbout S, Hsissou R, Erramli H et al. Gravimetric, electrochemical and theoretical study, and surface analysis of novel epoxy resin as corrosion inhibitor of carbon steel in 0.5 M H_2SO_4 solution. J Mol Struct. 2021;1245:131014. https://doi.org/10.1016/j.molstruc.2021.131014
31. Galai M, Rbaa M, Serrar H et al. S-Thiazine as effective inhibitor of mild steel corrosion in HCl solution: Synthesis, experimental, theoretical and surface assessment. Coll Surf A: Physicochem Eng Asp. 2021;613:126127. https://doi.org/org/10.1016/j.colsurfa.2020.126127
32. Bouckamp A. Users manual equivalent circuit. Fac Cheml Technol. 1993;(4).
33. Ouakki M, Galai M, Rbaa M et al. Electrochemical, thermodynamic and theoretical studies of some imidazole derivatives compounds as acid corrosion inhibitors for mild steel. J Mol Liq. 2020;319:114063. https://doi.org/10.1016/j.molliq.2020.114063

34. Balbo A, Frignani A, Grassi V et al. Corrosion inhibition by anionic surfactants of AA2198 Li-containing aluminium alloy in chloride solutions. Corros Sci. 2013;73:80-88. https://doi.org/ 10.1016/j.corsci.2013.03.027
35. Macdonald J. Emphasizing solid materials and systems. Impedance Spectroscopy. John Wiley & Sons Inc.: New York, NY, USA, 1987.
36. Hsissou R, El Harfi A. Application of Pentaglycidyl ether Penta-ethoxy Phosphorus Composites Polymers Formulated by Two Additives, Trisodium Phosphate (TSP) and Natural Phosphate (NP) and their Combination in the Behavior of the Coating on E24 Carbon Steel in NaCl 3. 5%.Analyt Bioanalyt Electrochem. 2018;10:728-738.
37. Hsissou R, Abbout S, Berisha A et al. Experimental, DFT and molecular dynamics simulation on the inhibition performance of the DGDCBA epoxy polymer against the corrosion of the E24 carbon steel in 1.0 M HCl solution. J Mol Struct. 2019;1182:340-351. https://doi.org/10.1016/j.molstruc.2018.12.030
38. Hsissou R, Dagdag O, Abbout S et al. Novel derivative epoxy resin TGETET as a corrosion inhibition of E24 carbon steel in 1.0 M HCl solution. Experimental and computational (DFT and MD simulations) methods. J Mol Liq. 2019;284:182-192. https://doi.org/10.1016/j.molliq.2019.03.180
39. Dagdag O, Hsissou R, Berisha A et al. Polymeric-based epoxy cured with a polyaminoamide as an anticorrosive coating for aluminum 2024-T3 surface: experimental studies supported by computational modeling. J Bio- Tribo-Corros. 2019;5:1-13. https://doi.org/10.1007/s40735-019-0251-7
40. Hsissou R, Benhiba F, Abbout S et al. Trifunctional epoxy polymer as corrosion inhibition material for carbon steel in 1.0 M HCl: MD simulations, DFT and complexation computations. Inorg Chem Commun. 2020;115:107858. https://doi.org/10.1016/j.inoche.2020.107858
41. Boucherit L, Al-Noaimi M, Daoud D et al. Synthesis, characterization and the inhibition activity of 3-(4-cyanophenylazo)-2,4-pentanedione (L) on the corrosion of carbon steel, synergistic effect with other halide ions in 0.5 M H2SO4. J Mol Struct. 2019;1177:371-380. https://doi.org/10.1016/j.molstruc.2018.09.079
42. El-Raouf AM, Khamis EA, Abou Kana AMTH et al. Electrochemical and quantum chemical evaluation of new bis(coumarins) derivatives as corrosion inhibitors for carbon steel corrosion in 0.5 M H_2SO_4. J Mol Liq. 2018;255:341-353. https://doi.org/10.1016/j.molliq.2018.01.148
43. El-Kholy AE, El-Taib HF. Electrochemical measurements and semi-empirical calculations for understanding adsorption of novel cationic Gemini surfactant on carbon steel in H_2SO_4 solution. J Mol Struct. 2028;1156:473-482. https://doi.org/10.1016/j.molstruc.2017.12.003
44. Hmamou DB, Salghi R, Zarrouk A et al. Investigation of corrosion inhibition of carbon steel in 0.5 M H_2SO_4 by new bipyrazole derivative using experimental and theoretical approaches. J Environm Chem Eng. 2015;3:2031-2041. https://doi.org/10.1016/j.jece.2015.03.018
45. Kowsari E, Payami M, Amini R et al. Task-specific ionic liquid as a new green inhibitor of mild steel corrosion. Appl Surf Sci. 2014;289:478-486. https://doi.org/ 10.1016/j.apsusc.2013.11.017

46. Hsissou R, Abbout S, Benhiba F et al. Insight into the corrosion inhibition of novel macromolecular epoxy resin as highly efficient inhibitor for carbon steel in acidic mediums: Synthesis, characterization, electrochemical techniques, AFM/UV–Visible and computational investigations. J Mol Liq. 2021;337: 116492. https://doi.org/10.1016/j.molliq.2021.116492
47. Musa A, Kadhum A, Mohamad B et al. Corros Sci. 2010;52:3331.
48. Bentiss F, Outirite M, Traisnel M et al. Improvement of corrosion resistance of carbon steel in hydrochloric acid medium by 3, 6-bis (3-pyridyl) pyridazine. Int J Electrochem Sci. 2012;7:1699-1723.
49. Emregül KC, Hayvalí M. Studies on the effect of a newly synthesized Schiff base compound from phenazone and vanillin on the corrosion of steel in 2 M HCl. Corros Sci. 2006;48:797-812. https://doi.org/10.1016/j.corsci.2005.03.001
50. Benabdellah M, Souane R, Cheriaa N et al. Synthesis of calixarene derivatives and their anticorrosive effect on steel in 1 M HCl. Pigm Res Technol. 2007. https://doi.org/10.110 8/03699420710831791
51. Marušić K, Ćurković HO, Takenouti H. Inhibiting effect of 4-methyl-1-p-tolylimidazole to the corrosion of bronze patinated in sulphate medium. Electrochim Acta. 2011;56:7491-7502. https://doi.org/10.1016/j.electacta.2011.06.107
52. Bentiss F, Lebrini M, Lagrene M et al.The Influence of Some New 2, 5-Disubstituted 1, 3, 4-Thiadiazoles on the Corrosion Behaviour of Mild Steel in 1 M HCl Solution: AC Impedance Study and Theoretical Approach. Electrochim Acta. 2007;52:6865-6872. https://doi.org/10.1016/j.electacta.2007.04.111
53. Alaoui K, Kacimi YE, Galai M et al.Poly (1-phenylethene): as a novel corrosion inhibitor for carbon steel/hydroc hloric acid interface. Analyt Bioanalyt Electrochem. 2016:830-847.
54. Hassan HH. Perchlorate and oxygen reduction during Zn corrosion in a neutral medium. Electrochim Acta. 2006;51:5966-5972. https://doi.org/10.1016/j.electacta.2006.03.065
55. Verma C, Quraishi M, Obot I et al. Effect of substituent dependent molecular structure on anti-corrosive behavior of one-pot multicomponent synthesized pyrimido [2, 1-B] benzothiazoles: computer modelling supported experimental studies. J Mol Liq. 2019;287:110972. https://doi.org/10.1016/j.molliq.2019.110972
56. Ech-Chihbi E, Nahlé A, Salim R et al. Computational, MD simulation, SEM/EDX and experimental studies for understanding adsorption of benzimidazole derivatives as corrosion inhibitors in 1.0 M HCl solution. J Alloys Comp. 2020;844:155842. https://doi.org/10.1016/j.jallcom.2020.155842
57. Alaoui K, El Kacimi Y, Galai M et al. Poly (1-phenylethene): as a novel corrosion inhibitor for carbon steel/hydrochloric acid interface. 2016:830-847.
58. Alaoui K, El Kacimi Y, Galai M et al. Anti-corrosive properties of polyvinyl-alcohol for carbon steel in hydrochloric acid media: Electrochemical and thermodynamic investigation. J Mater Environ Sci. 2016;7:2389-2403.
59. Boumezzourh A, Ouknin M, Chibane E et al. Inhibition of tinplate corrosion in 0.5 M $H_2C_2O_4$ medium by *Mentha pulegium* essential oil. Int J Corros Scale Inhib. 2020;9(1):152-170. https://doi.org/10.17675/2305-6894-2020-9-1-9
60. Dahmani K, Galai M, Ouakki M et al. Corrosion inhibition of copper in sulfuric acid via environmentally friendly inhibitor (*Myrtus communis*): Combining experimental and theoretical methods. J Mol Liq. 2022;347:117982. https://doi.org/10.1016/j.molliq.2021.117982